Mine Water and the Environment (2018) 37:249–262
https://doi.org/10.1007/s10230-018-0533-1

TECHNICAL ARTICLE

Multivariate Analysis of Water Quality of the Chenqi Basin, Inner Mongolia, China

Honglei Liu[1,2,3] · Qiang Wu[1,2] · Mingjun Wang[4] · Meng Zhang[2]

Received: 18 July 2017 / Accepted: 12 March 2018 / Published online: 19 March 2018

Abstract

Numerous water samples are necessary to predict and assess water quality. However, if the geographical conditions surrounding mines are harsh mountainous areas, continuous or uniform sampling can be challenging, resulting in difficult sampling or data loss. In this study, statistical analysis of normalized data collected in the Chenqi Basin, including factor analysis and principal component analysis, revealed the water quality's macro-distribution. Analytic solutions of partial differential equations of regional phreatic water quality were used to evaluate the mining and recharge–discharge of the regional phreatic aquifer. This method compensates for the disadvantage of evaluating discrete samples. Hydrogeological monitoring, pumping tests, and water quality analysis of phreatic water were carried out in the west of the Dongming open pit mine. Eight hydrogeochemical water quality variables (WQV) were selected as analysis targets. With hydrogeological generalization, regression equations of the diffusion of WQV and the seepage field were developed by a cumulative index that samples data from different orientations. One-dimensional diffusion partial differential equations of WQV, which are related to the distance and time of the seepage flow, were derived. Current and future predictions and evaluations of the phreatic water quality in the basin were made by ArcGIS based on regression and cumulative evaluation index methods. Findings revealed that the influence area of the mine would significantly expand in 10 years if current conditions continue. In addition, the diffusion speed was found to be higher in the southwestern part of the mine than in the west and northwestern parts, which is consistent with the recharge and discharge conditions of the Chenqi Basin.

Keywords Mine water environment · Phreatic water · Water quality evaluation · Water quality prediction · Water quality variables · Open-pit mine

Introduction

In northern China, groundwater is not only an important source of water supply but also closely related to the health of residents (Li et al. 2016). Since the 1990s, the groundwater has been affected by mining, especially by open-pit mining, and is polluted to various degrees, causing environmental problems (Li 2016). Expanded regulation of the water table's response to mining, and exploring the relationship between the time and space of hydrogeochemical water quality variables (WQV) are viewed as promising and useful strategies to evaluate and predict mine water's environmental effects (Li et al. 2014; Senapaty et al. 2012).

Groundwater sampling involves a considerable amount of fieldwork and continuous or uniform sampling. Large numbers of water samples are the primary data source for water quality evaluation (Andrade et al. 2017; Noble et al. 2016). Methods for evaluating such coal mine phreatic water quality data include the single-factor index, Nemerow index, fuzzy comprehensive evaluation, analytic hierarchy process, artificial neural network, principal component analysis (PCA), gray evaluation method, and genetic algorithm (Li et al. 2013; Qian et al. 2016). However, sometimes, it can be very difficult to collect water samples in a mining area.

✉ Honglei Liu
liuhonglei@student.cumtb.edu.cn

[1] National Engineering Research Center of Coal Mine Water Hazard Controlling, China University of Mining and Technology (CUMTB), Beijing, China

[2] School of Geoscience and Surveying Eng, CUMTB, Beijing, China

[3] Illinois State Geological Survey, University of Illinois at Urbana-Champaign, Champaign, USA

[4] Mine Section, Institute of Geo-environmental Monitoring of Inner Mongolia Autonomous Region, Hohhot, China

For example, appropriate sampling sites may be occupied by industrial sites or a labor and management shortage may interrupt sampling. In such instances, conventional evaluation methods will not work. This study was conducted in a region in northeastern Inner Mongolia, where the adverse geomorphic conditions in and around some coal mines of the Chenqi Basin made it difficult to consistently collect phreatic water quality samples. PCA was used to resolve this problem.

Hydrogeological Environment of the Chenqi Basin

The eastern and northern parts of the study area are the low mountainous and hilly area of the Greater Khingan Range, and the southern part is the Hulun Buir Plain. The Chenqi Basin is situated in the transitional region between these two areas (Fig. 1). Thus, the altitude is high in the north and east, and relatively low in the south and west.

Situated in the mid-latitude region, the study area has a temperate continental semi-arid climate. This area belongs to the Eerguna River watershed, in which the Mergel and Argun Rivers are the two main rivers. The average annual precipitation in the study area is approximately 347 mm, 60% of which is concentrated in August. The average annual evaporation is 1285 mm, and the maximum rainfall is 86 mm in 24 h.

The study area lies in the northeast of the Hailar Basin Group; its fourth-order tectonic unit is the Chenqi Basin. The regional structures of the area include the: Hailar River Fault (the southern boundary of the Chenqi Basin), Touzhan Fault (northern boundary), Kuku Fault (western boundary), and Dongdagou Fault (eastern boundary). In terms of stratigraphic units, the Chenqi Basin is dominated by low Carboniferous metamorphic rock formations (C_1), low Cretaceous Longjiang formations (K_1l), Damohe (K_1d), Pleistocene, and Holocene formations (Q_{2+3}, Q_4) (Fig. 2).

The Chenqi Basin, which is a large phreatic water resource, contains the Quaternary Holocene alluvial layer, the upper and middle Pleistocene ice layer, and the alluvial–lacustrine deposits. The thickness of the phreatic aquifer is 10–40 m, and single well inflows range from 1000 to 3000 m^3/d. The depth to the groundwater table is 5–25 m and its hydrochemical type is HCO_3-Na·Ca. The salinity of the phreatic water is low, ranging from 130 to 910 mg/L. The phreatic aquifer is mainly subjected to infiltration of atmospheric precipitation and ephemeral seepage recharge from the river, which is heavily influenced by the drainage of the Dongming (D.M.) open pit mine, thereby forming an irregular circular cone of depression.

According to an analysis of the groundwater flow field during dry and rainy periods from 2014 to 2015, the phreatic water of the Chenqi Basin is mainly recharged by rainfall infiltration and river water. Water draining from other mines affects the eastern portion of the basin and flows to the D.M. mine, while the western portion discharges to Chagan Lake. The upper, middle, and lower sections of the Mergel and Argun Rivers were investigated from July to August 2015; both rivers, as well as the downstream lake, are groundwater drainage channels.

Water discharge at the initial stage of the D.M. mine operation was ≈273,200 m^3/d (from 2007 to 2008), and stabilized at ≈107,700 m^3/d (from 2013 to 2014). In 2014, sampled fracture water in the coal strata and Quaternary interstitial water showed that the water level of phreatic

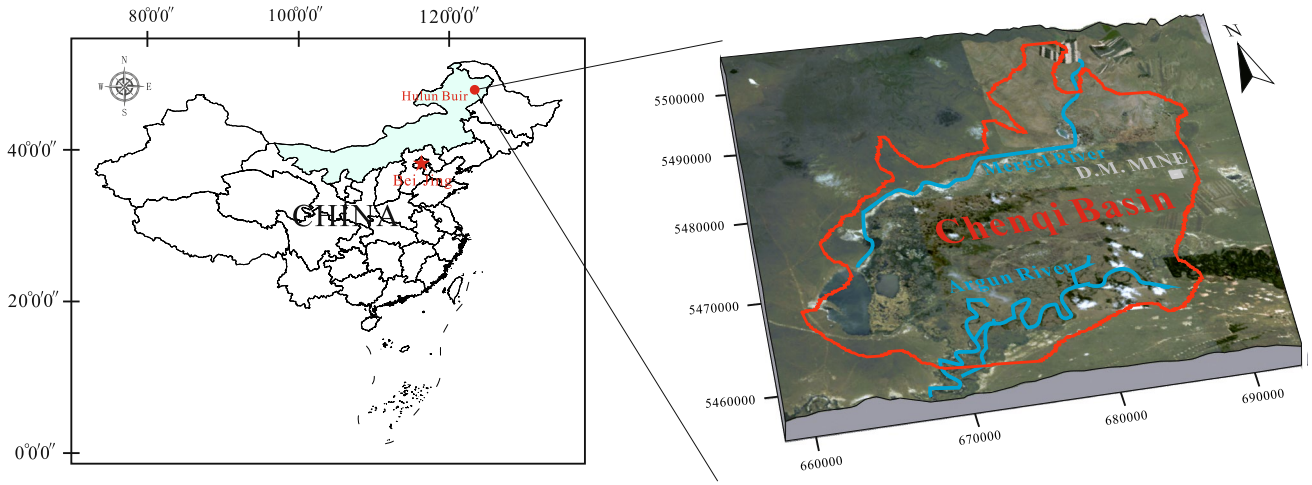

Fig. 1 Geographic and geomorphic map of the study area

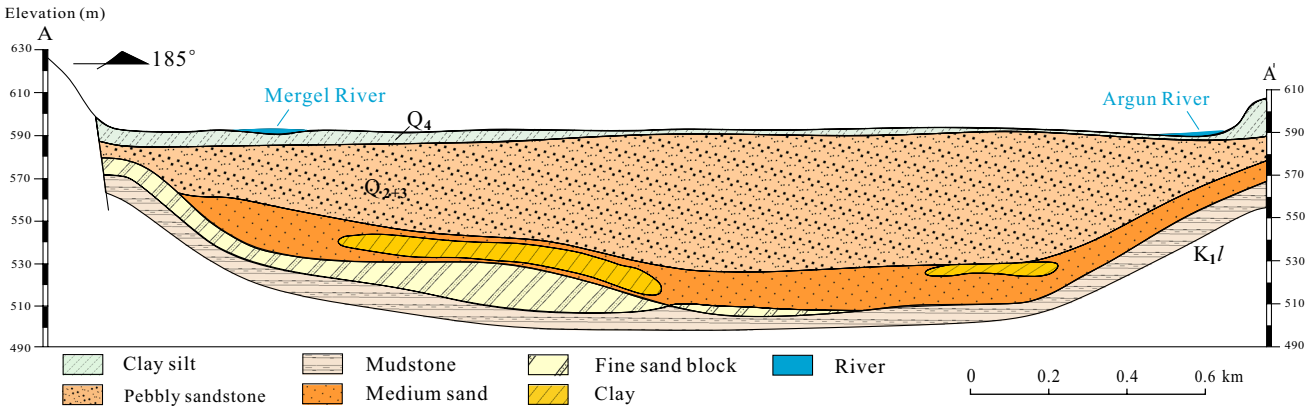

Fig. 2 Geological section map of the study area

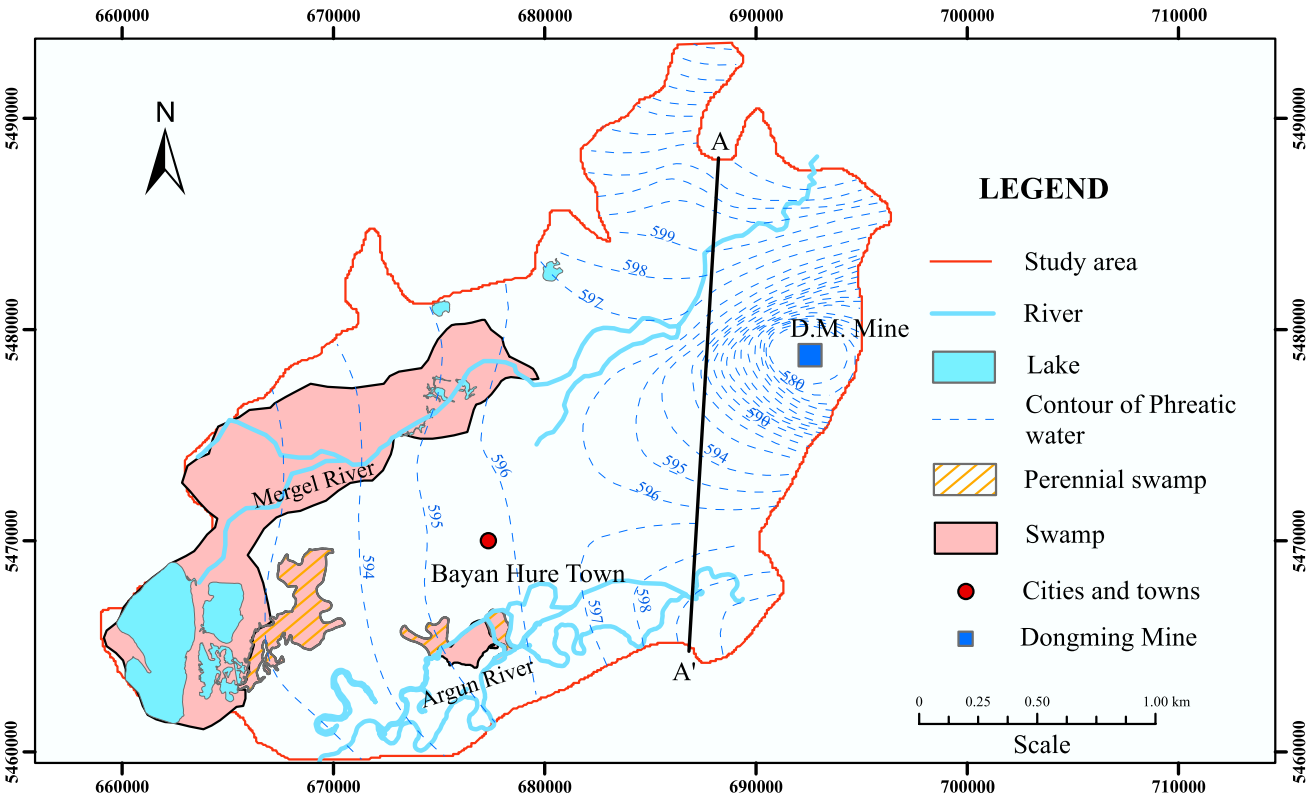

Fig. 3 Contour map of phreatic water level of the study area

water in the western Chenqi Basin was higher than the upper level of phreatic water in the coal-bearing strata.

The cone of depression formed by mining (Rapantova et al. 2007; Sun et al. 2015) ensures the safety and security of mining by reducing the water level and pressure in the mine. In Fig. 3, the phreatic water level in the Chenqi Basin is influenced by the mine; the cone of depression extends 1.5–2.0 km from the mine, with the hydraulic gradient decreasing with distance. Cones of depression change groundwater flow but can also lead to groundwater quality deterioration and even pasture degradation (Chai 1981; Li et al. 2017; Lu et al. 2006).

Materials and Methods

Samples and data were collected in wells that could be accessed in the chenqi basin. Factor analysis and PCA were used to interpret the normalized index tendency of 12 water samples based on hydrochemical WQV that exceeded the relevant standards for drinking water. The cumulative evaluation index is calculated by analytical solutions of the partial differential equation of the phreatic water and was used to this study. The regression equation of the normalized index and the solution of the partial equation were combined to evaluate and predict the water quality in the chenqi basin. This approach determines the time–space relationship of the water quality in the area and fills the gap between the sampling data and water quality evaluation.

Sampling and Analysis

Systematic groundwater sampling was carried out in May 2015. Representative water samples (temporal and spatial distribution of phreatic water samples) were collected from 12 0.5–20 m deep wells in the Chenqi Basin (Fig. 4). They were all collected in 550 mL narrow-mouth pre-washed high-density polyethylene bottles (Qian et al. 2016; Yihdego et al. 2016). NH_4^+, Cl^-, SO_4^{2-}, NO_3^-, total hard (TH), total dissolved solid (TDS), Mn^{2+}, and chemiluminescent detection of the permanganate index (COD_{Mn}) were selected as the eight WQV, based on the National Standards for Drinking Water Quality in China (GB 5749-2006). The samples can be divided into three groups, based on their location and direction from the mine: Line A (northwest), Line B (west), and Line C (southwest). Thus, four sampling points existed in each direction at a distance of 300–330 m from each other.

At the sampling sites, bottles were again washed with the sampled water prior to sample collection, and bubbles were prevented from entering (Michael et al. 2016). Three bottles were collected at each point, and all of the samples were sealed with plastic film. The values of pH, TDS, total hardness (TH), [NH_4^+], [Mn^{2+}], and [COD_{Mn}] ([] indicates concentrations) were measured in the field (Orion AQ3700). The [NO_3^-, Cl^-, and SO_4^{2-}] were measured by ion chromatography (Dionex, DX-120) 4–10 days after sampling. No less than 5% was sampled to monitor the sampling quality. Then, the sample was added to the standard water samples according to the proportion. Repeated and blank samples were randomly sampled, and 20% were re-analysed to ensure

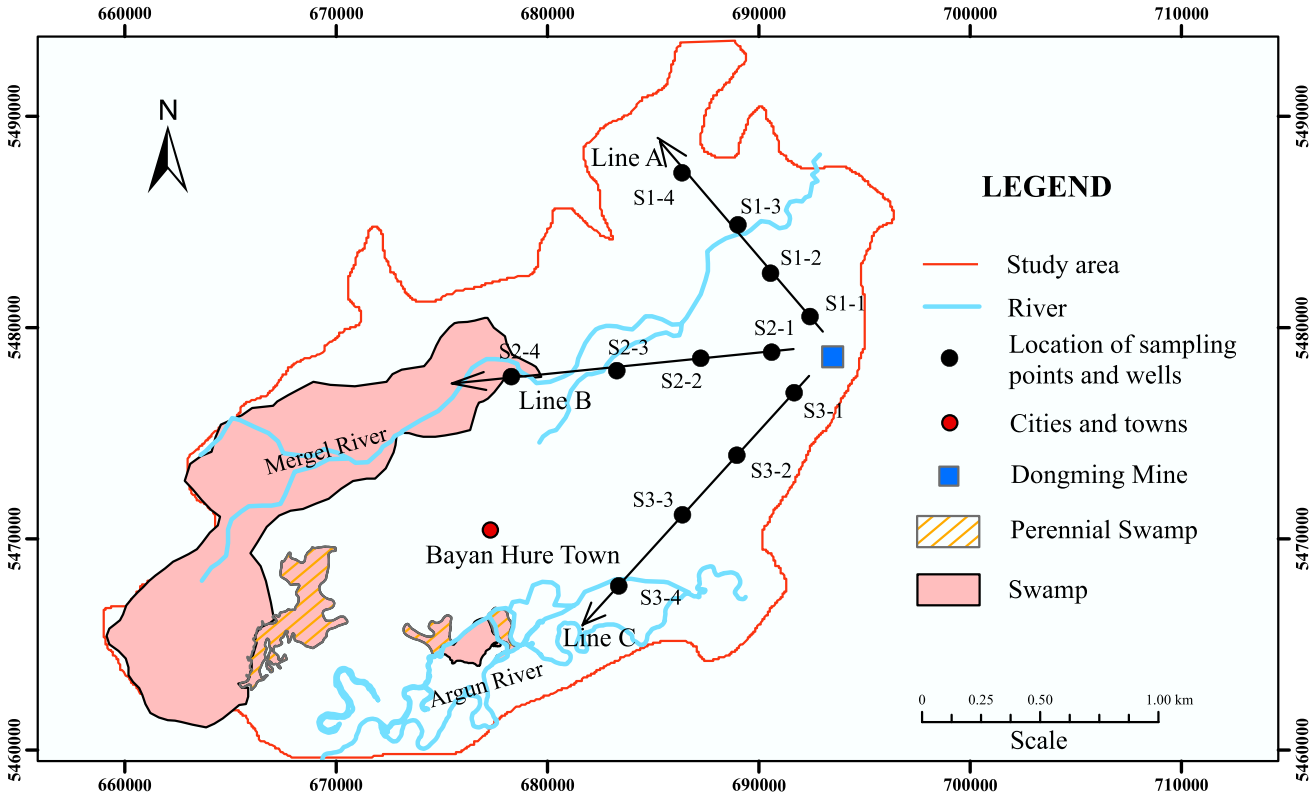

Fig. 4 Map of wells and sampling points in the study area

that the relative deviation passing rate of each batch was not less than 90%.

The test results were checked by calculating the anion-cation balance; the relative error of most of the water samples was within 5%. High-salinity water samples were controlled within 10%.

Statistical Analysis

Multivariate statistical methods were used to investigate and interpret the hydrogeochemical data, to establish relationships between the data (Bencer et al. 2016; Ling et al. 2017; Mohammad et al. 2017), to reveal the process that generated the observed water compositions (Fijani et al. 2017; Rajmohan et al. 2017; Wu et al. 2014). The combined use of factor analysis and PCA is an effective means of manipulating, interpreting, and representing hydrogeochemical data (Houillon et al. 2016; Jiries et al. 2004; Lamhonwah et al. 2017). The data transformation technique of PCA attempts to reveal a simple underlying structure, which is assumed to exist within a multivariate data set (Balintova et al. 2016; Noble et al. 2016).

In this study, PCA was used to select the WQV that exceeded the National Standards for Drinking Water Quality in China, to explain the source of the groundwater recharge according to the trend of WQV. All of the multivariate analyses were performed using Statistical Product and Service Solutions (SPSS) version 21.0. In addition, an orthogonal polynomial fitting curve was drawn to analyse the error between the observed data and the mathematical fitting model, as well as the cause of the abnormal trend and curve variation.

Prior to statistical analyses, all of the data collected were normalized using Formula 1. Normalized WQV data tend to minimize the impact of the difference of variance in variables, thereby rendering the data dimensionless. When data range from $c_{\min}$ to $c_{\max}$, the formula of the normalized index data is:

$$\hat{Y}_i = \sum \frac{c_i - \min(c_j)}{\max(c_j) - \min(c_j)}. \tag{1}$$

Then, the effect of the cumulative statistical index and evaluation methods in the environment can be determined.

Cumulative Evaluation Index (CEI) of the Phreatic Water Quality

According to Fickle's law and mass conservation, the saturated one dimensional (1D) uniform flow is included in a 1D steady flow and 1D convection–diffusion migration process (Lu et al. 2006; Mahato et al. 2016), respectively, Formula 2:

$$\begin{cases} \frac{\partial c}{\partial t} = \xi_L \frac{\partial^2 c}{\partial x^2} - u\frac{\partial c}{\partial x} & \\ c(x,0) = 0 & 0 \leqslant x < \infty \\ c(0,t) = c_0 & t > 0 \\ c(\infty,t) = 0 & t > 0 \end{cases}. \tag{2}$$

The analytic solution of the partial differential equation (Formula 3) is obtained by Laplace transformation:

$$c(x,t) = \frac{c_0}{2} erfc\left(\frac{x-ut}{2\sqrt{\xi_L t}}\right) + \frac{c_0}{2}\exp\left(\frac{ux}{\xi_L}\right) erfc\left(\frac{x-ut}{2\sqrt{\xi_L t}}\right) \tag{3}$$

where $c(x,t)$ is the normalized index of the water quality variable in the sample point and is x m away from the mining area at a certain time; c_0 is the normalized index of the water quality variable in the imaginary center of the mining area; u is the average velocity of the phreatic water flow, m/d; ξ_L is the hydrodynamic dispersion coefficient of Chenqi Basin, where the measured ξ_L is 1.5120 m^2/d according to in situ testing; and x is the distance from the imaginary center of the mining area.

It is anticipated that the D.M. Mine will continue operating for 30 years based on its coal reserves. Thus, the second part of the analytic solution is considerably less than the first and can be omitted in this condition. Accordingly, when the phreatic flow field is stable in the study area, the analytic solution of the partial differential equations is simplified as Formula 4:

$$c(x,t) \approx \frac{c_0}{2}\mathrm{erfc}\left(\frac{x-ut}{2\sqrt{\xi_L t}}\right). \tag{4}$$

In analysing the storage of phreatic aquifer, the effects of precipitation, and the Mergel River water on recharge, evaporation, and other water sources were considered. The weighting coefficient of a certain source affects water quality (Formula 5):

$$\lambda_m = Q_m / \sum_{i=i}^{n} Q_i, \tag{5}$$

where λ_m is the weight for the water quality affected by different water flow; Q_m is the amount of recharge and discharge source; $\sum_{i=i}^{n} Q_i$ is the total amount of source. The relation between the seepage and the actual velocity (Formula 6) is:

$$u = \frac{v}{\varepsilon} = \frac{KI}{\varepsilon}, \tag{6}$$

where K is the permeability coefficient of the phreatic aquifer; I is the hydraulic gradient; ε is the effective porosity of

phreatic aquifer; and $\varepsilon = 0.3$ in Chenqi Basin. The normalized index of the WQV was calculated using Formulas 7 and 8:

$$C(x,t) = \sum_{i=1}^{n} |\lambda_i| c_i(x,t) = \sum_{i=1}^{n} \left[|\lambda_i| \frac{c_{i0}}{2} erfc\left(\frac{x-ut}{2\sqrt{\xi_L t}} \right) \right], \tag{7}$$

Formulas 7 is derived from Formulas 4 and 5, which is the cumulative superposition of the WQV of each sampling point with time and position changing in the study area.

$$\begin{aligned} \lambda_i &= K_i I_i \Delta H_i \left(\sum_{i=1}^{j} Q_i \right)^{-1} = \overline{v}(x,t) \Delta H_i \left(\sum_{i=1}^{j} Q_i \right)^{-1} \\ &= u \Delta H_i \left(n \sum_{i=1}^{j} Q_i \right)^{-1}. \end{aligned} \tag{8}$$

Formulas 8 is a variant of Formula 5, and is based on Formula 6 and the relationship between groundwater flow velocity and the thickness of the unconfined aquifer. In this case, $\triangle H$ is the average thickness of the phreatic aquifer. Based on Formulas 7 and 8

$$C(x,t) = \sum_{i=1}^{n} \left[c_{i0} u \Delta H_i \left(2n \sum_{i=1}^{j} Q_i \right)^{-1} \mathrm{erfc}\left(\frac{x-ut}{2\sqrt{\xi_L t}} \right) \right], \tag{9}$$

According to the definition of the normalized index data by Formula 1, $\hat{Y}(x,t)$, the cumulative evaluation index can be stated as Formula 10.

$$\widehat{Y}(x,t) \approx \sum_{i=1}^{n} \left(\frac{c(x,t) - c_{\min}}{c(x_0,0) - c_{\min}} \right). \tag{10}$$

Then, take $C(x,t)$ of Formula 9 into Formula 10. The cumulative evaluation index of the research area is calculated, which is related to both the distance and the duration of effective time.

$$\begin{aligned} \widehat{Y}(x,t) \approx \sum_{i=1}^{n} \Bigg\{ \sum_{i=1}^{n} \left[c_{i0} u \Delta H_i \left(2\varepsilon \sum_{i=1}^{j} Q_i \right)^{-1} \mathrm{erfc}\left(\frac{x-ut}{2\sqrt{\xi_L t}} \right) \right] \\ \left(c_{i0} - c_{\min} \right)^{-1} - c_{\min} \left(c_{i0} - c_{\min} \right)^{-1} \Bigg\}. \end{aligned} \tag{11}$$

Next, the spatial covariance of the optimal interpolation method, namely the Kriging interpolation method, is used to express and evaluate the water quality of the isolated point data. According to Formula 11, $\hat{Y}(x,t)$, the cumulative evaluation index is related to the distance from the mine (x) and the duration of exploration (t). So, Kriging was used with 2D spatial representation by Esri ArcGIS for desktop 10.3.1 to classify the phreatic water quality into five categories (Table 1):

Table 1 Classification of water quality and range of $\hat{Y}(x,t)$

Water quality	I	II	III	IV	V
$\hat{Y}(x,t)$	< 1.00	1.00–< 2.00	2.00–< 3.00	3.00–< 4.00	> 4.00

(I): $\hat{Y}(x,t)$ is close to the natural background content and suitable for a variety of uses;

(II): $\hat{Y}(x,t)$ is slightly higher than natural background but the water is still suitable for all uses;

(III): $\hat{Y}(x,t)$ is suitable as a drinking water source, water supply, and agricultural water consumption;

(IV): $\hat{Y}(x,t)$ meets the requirements of industrial and agricultural water and can be used as drinking water after appropriate treatment;

(V): Unsuitable for drinking.

Results and Discussion

Chemical Composition of the Chenqi Basin Phreatic Water

The hydrogeochemical analysis of phreatic water samples collected from different areas of the Chenqi Basin is given in Table 2. The physical properties of the phreatic water samples varied with distance from the D.M. Mine. Some of the samples near the mine were pale, lemon, or yellow in colour, with a fishy smell and slightly turbid. However, most of the samples from the area were colorless, tasteless, odorless, and transparent.

The pH of the samples ranged from 6.52 to 8.12, averaging 7.02. In Line A, sampling points S1-2 and S1-3 have the same pH, 7.66. However, a water divide is located between S1-3 and S1-4, which indicates that the pH is influenced by the water of both the phreatic aquifer and river water recharge. The COD_{Mn} decreased from 4.16 to 1.1 in the sampling wells further away from the mine. The [NO_3^-] indicated an organic pollutant in the phreatic zone. Like the [COD_{Mn}], the [NO_3^-] of the first two sampling points in Lines A, B, and C also decreased away from the D.M. Mine.

Spatial variations in TH and TDS were observed in the mine water samples. If the fourth (most distant) sampling points in Lines A, B and C are assumed not to be affected by the D.M. Mine, [TH] decreased with distance from the mine. In addition, relatively high [TDS] were observed in S2-2 while low values were found in S2-3. Also, [TDS] in S2-1 to S2-4 were less than in Lines A and C. The difference in [TDS] and spatial variability may reflect variations in the coal seams and associated geological formations, as

Table 2 Hydrochemical parameters of phreatic water samples in Chenqi Basin (mg/L)

Line	Sample number (distance from mine)	NH_4^+	Cl^-	SO_4^{2-}	NO_3^-	TH	TDS	Mn^{2+}	COD_{Mn}	pH
Line A	S1-1	0	38.29	17.77	1.91	182.66	474.86	0.52	4.16	6.86
	S1-2	0.04	37.23	13.45	0.46	65.06	367.84	0	1.58	7.66
	S1-3	0.02	10.64	61.48	0	230.21	372.6	0.52	1.1	7.66
	S1-4	0.77	8.86	12.97	0	167.65	267.6	0.32	4.37	6.68
Line B	S2-1	0	101.04	138.33	1.06	352.32	809.86	2	3.31	6.52
	S2-2	0	124.09	139.29	0.86	310.28	927.58	0.04	11.07	8.12
	S2-3	0.12	3.55	0	2.52	66.06	115.58	0.93	2.53	7.02
	S2-4	0.08	7.09	0	2.42	77.57	126.84	0	1.82	6.94
Line C	S3-1	0.43	11.34	24.02	3.25	332.8	580.93	0.69	3.53	7.38
	S3-2	0.03	35.45	58.6	3.31	296.27	444.62	0.16	3.29	6.82
	S3-3	0.27	11.34	19.21	0	289.26	497.84	0.9	5.79	7.04
	S3-4	0.08	8.86	11.05	1.15	207.18	349.32	0.24	3.56	7.78

well as the mining and hydrogeological conditions created by the cone of depression. The [Cl^-, COD_{Mn}, and TH] in the water samples were generally in agreement, except for a few sampling sites. The [Cl^-] of sampling points S1-4, S2-4, and S3-4 are approximately the same and are close to the background values in the Chenqi Basin's geohydrological files, which strongly supports the assumption above. Additionally, the [SO_4^{2-} and NO_3^-] show a similar tendency, while the [NH_4^+ and Mn^{2+}] were close to the study area's background values, according to regional records. Moreover, [NH_4^+] of S1-1 and S2-1 are zero, indicating that the [NH_4^+] are not caused by the D.M. Mine.

Multivariate Statistical Analysis

According to Formula 1, the correlation coefficient matrix (Table 3), eigenvalue, and contribution rate (Table 4), and the coefficient matrix of principal components (Table 5) were listed using the commercial statistical software, SPSS for Windows. Table 3 shows the correlation coefficients of the phreatic water normalized index in the Chenqi Basin. As shown in Table 3, [Cl^-] is positively correlated with the [SO_4^{2-}, TDS, and COD_{Mn}], indicating the continuous addition of these variables along the groundwater flow path. In addition, the [SO_4^{2-}, TDS, and TH] are positively correlated. TDS is likely to show an increasing trend from upstream to downstream in a given hydrogeological unit due to mineral dissolution. NH_4^+ is insignificantly correlated with Cl^- or SO_4^{2-}, again indicating that NH_4^+ is likely not originating in the D.M. Mine.

Table 4 summarizes the results from our analysis, including the variables of the first three principal components, which have eigenvalues greater than 1. The three significant components altogether explained 80.05% of the total variance of the data.

As shown in Table 5, Component 1 accounts for approximately 49.9% of the total variance and has large SO_4^{2-}, Cl^-, and TDS loadings. This component also indicates that the increased [TDS] in the groundwater of the Chenqi Basin may be due to the D.M. Mine. Component 2 accounts for 15.7% of the total variance and has high NH_4^+ and COD_{Mn} loadings, which show that the Chenqi Basin's groundwater may be influenced by industrial waste, which may be related to the mining process. Component 3 shows that 14.4% of the total variance correlates with Mn^{2+}, which indicates that

Table 3 Correlation coefficients matrix of the water quality variables of Chenqi Basin

Excessive factors	NH_4^+	Cl^-	SO_4^{2-}	NO_3^-	TH	TDS	Mn^{2+}	COD_{Mn}
NH_4^+	1.000							
Cl^-	− 0.413	1.000						
SO_4^{2-}	− 0.363	0.904	1.000					
NO_3^-	− 0.156	− 0.125	− 0.162	1.000				
TH	0.007	0.488	0.683	0.025	1.000			
TDS	− 0.225	0.860	0.860	− 0.133	0.811	1.000		
Mn^{2+}	− 0.025	0.223	0.362	− 0.049	0.422	0.319	1.000	
COD_{Mn}	0.044	0.636	0.519	− 0.172	0.468	0.677	− 0.104	1.000

Table 4 Eigenvalue and contribution rate of water quality variables

Component	Initial eigenvalues			Extraction sums of squared loading		
	Total	Variance/ %	Cumulative/ %	Total	Variance/ %	Cumulative/ %
1	3.996	49.948	49.948	3.996	49.948	49.948
2	1.252	15.650	65.599	1.252	15.650	65.599
3	1.156	14.447	80.046	1.156	14.447	80.046
4	0.927	11.589	91.635			
5	0.340	4.247	95.882			
6	0.230	2.874	98.755			
7	0.091	1.131	99.887			
8	0.009	0.113	100.000			

Table 5 Matrix of principal components' coefficients

Factors	Component		
	1	2	3
NH_4^+	− 0.296	0.783	0.361
Cl^-	0.911	− 0.115	− 0.240
SO_4^{2-}	0.941	− 0.111	− 0.006
NO_3^-	− 0.156	− 0.627	0.053
TH	0.784	0.088	0.366
TDS	0.969	0.052	0.006
Mn^{2+}	0.376	−0.179	0.827
COD	0.689	0.422	−0.384

coal mining is the likely cause of the Chenqi Basin's high metal concentrations.

The trend (Fig. 5) of the normalized index of SO_4^{2-}, Cl^-, TDS, NH_4^+, COD_{Mn}, and Mn^{2+} in the coefficient matrix of the principal components was found to be associated with the role of the cumulative evaluation index (CEI) method and regression equation, as described below. Figure 5 generally shows a remarkable downward tendency with increasing distance from 300 to 1200 m. By contrast, NH_4^+ (Fig. 5d) showed a rising trend. Figure 5a–f reflects that six WQV presents a generally falling trend as the distance from the mine increased. However, numerous abnormal changes were observed in the curves.

COD_{Mn} is a representative indicator of water pollution. Figure 5c shows that the [COD_{Mn}] has an increasing tendency, ranging from 300 to 600 m. According to Fig. 1, the local gradient of the curve is formed by the increased hydraulic gradient near the mining area due to drainage of the mine. However, the normalized index curve of Fig. 5f reflects the double influence of background values and mining in the range, which forms an exponential rebound phenomenon in the range of 600–900 m.

SO_4^{2-} can reflect the flow of phreatic water. In Fig. 5b, although the phreatic water quality in the area is affected by mine drainage, no evident difference exists in the water flow velocity in the interior of the region. However, the normalized index trend in Fig. 5b, e are different from 600 to 900 m, which may be due to mining and mine drainage.

TDS is often used to indicate groundwater flow that has been influenced by the rock and soil solubility of the phreatic aquifer. When the value is high, the regional groundwater flow develops; conversely, the local groundwater flow develops. As shown in Fig. 5e, the TDS trend in different directions is consistent and indicates a positive correlation with the distance. At ≈500 m from the mining area, the [TDS] is between 350 and 900 mg/L, which shows that the Chenqi Basin's groundwater dynamic condition is good.

In general, the spatial patterns of water chemistry in different directions and the spatial distribution of WQV were similar, indicating that the water quality and recharge–discharge characteristics of the sampling sites were affected by the D.M. Mine. However, according to the cumulative index of normalized data in Fig. 6, the water chemical component anomaly and spatial variation in Line B (west direction) is greater than in Lines A and C. Figure 6 shows the different groundwater recharge characteristics in the north and south.

In the fitting curve of the three orthogonal polynomials with the cumulative index of the eight WQV, the form of the macro-regression equation is expressed as Formula 12:

$$\widehat{Y} = f(x_1, x_2, \cdots, x_m) = b_0 + b_1 x + b_2 x^2 + \cdots + b_m x^m. \quad (12)$$

Changes in the eight WQV in the phreatic aquifer are due to many factors. The cumulative index of WQV in Lines A, B, and C, as well as the other corresponding data recorded could determine the macro-regression equation of WQV within the mining area to evaluate and predict the distribution of WQV. The obtained predictive formula is shown in Table 6.

Quality Evolution of Mine Water by CEI

In the Chenqi Basin, the aquifer is composed of Quaternary unconsolidated rock phreatic pore water and capillary water. Nevertheless, no additional hydraulic relationship exists between the valley and the plain in the Chenqi Basin.

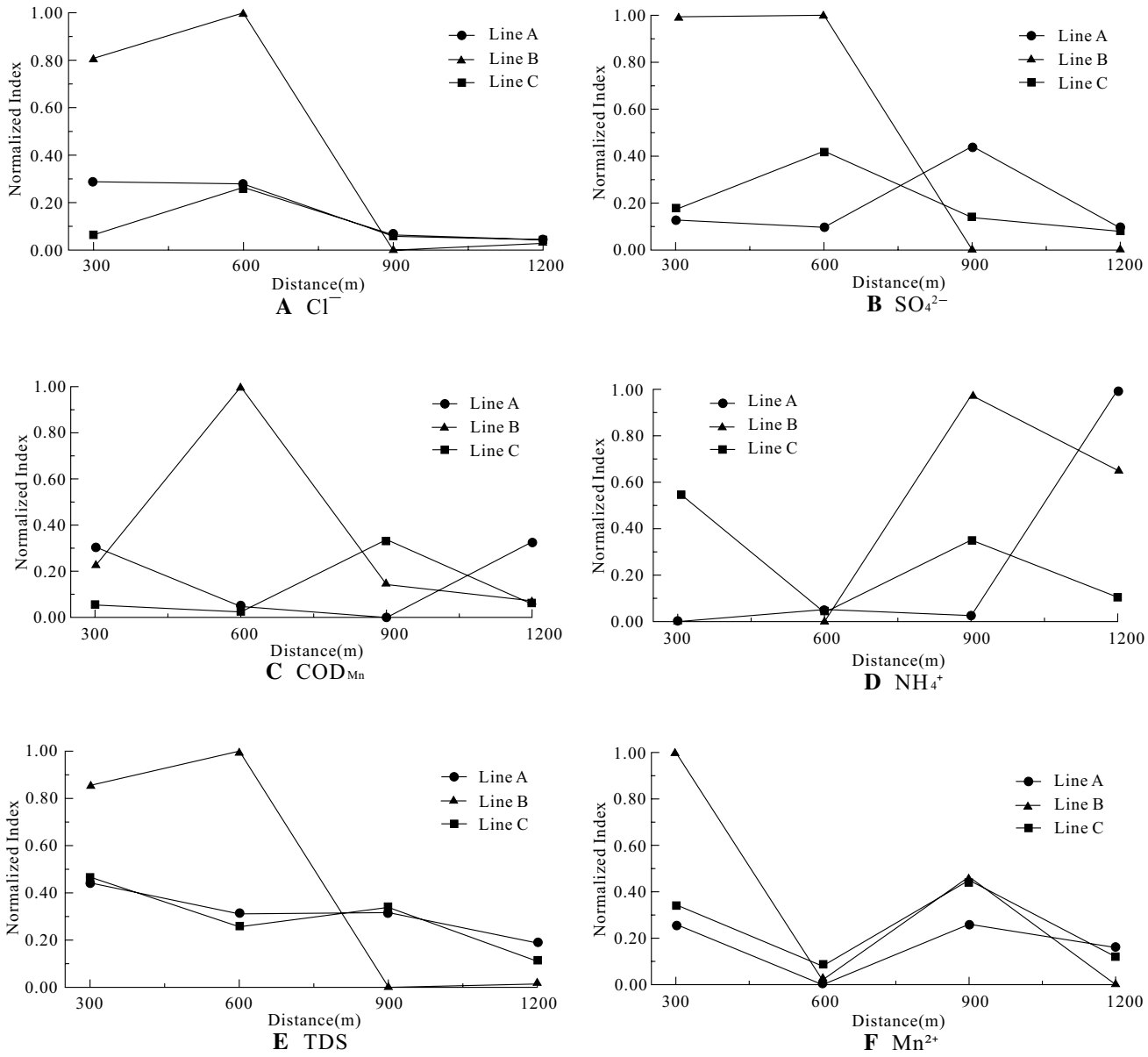

Fig. 5 Tendency chart of six water quality variables in the study area. **a** Cl^-. **b** SO_4^{2-}. **c** COD_{Mn}. **d** NH_4^+. **e** TDS. **f** Mn^{2+}

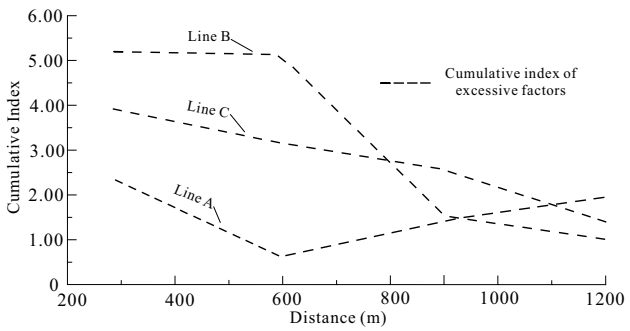

Fig. 6 Cumulative index of normalized data in Chenqi Basin

The groundwater balance is shown in Table 7. The phreatic water quality in the Chenqi Basin was evaluated by the CEI method. Given the short distance between the D.M. Mine and the Mergel and Argun Rivers (the direct distance is, at most, 1.5 km), the influence of the rivers on the phreatic water level and water quality cannot be ignored. The observed water levels show that river water affects the phreatic water contours and its pervasive orientation. Therefore, recharge of surface water or other sources and direction of water flow should be considered in analyzing the migration process. Figure 7a, b show the CEI results and the regression equation of the phreatic water evaluation in the Chenqi Basin based on the macro-regression equations of the three paths

Table 6 Macro-regression equations of various lines

Path	Macro-regression Equation	R^2
Line A	$\hat{Y}_{Line1} = 8.633 - 0.031x + 4.019x^2 - 1.542x^3$	0.9941
Line B	$\widehat{Y}_{Line2} = -4.884 + 0.058x - 9.309x^2 + 4.079x^3$	0.9965
Line C	$\widehat{Y}_{Line3} = -5.255 - 0.007x + 7.589x^2 - 3.822x^3$	0.9788

Table 7 The average annual groundwater balance in Chenqi Basin (2005–2015)

Factors of equilibrium	Water ($\times 10^8$ m^3/a)
Supply	
Precipitation recharge ($Q_{Recharge}$)	0.3793
Groundwater inflow (Q_{Inflow})	0.0298
River leakage ($Q_{R.Leakage}$)	0.2858
Discharge amount of drainage channel (Q_{Drain})	0.0120
Flood infiltration (Q_{Flood})	0.0972
Total (Q_{Supply})	0.8041
Excretion	
Groundwater evaporation ($Q_{Evaporation}$)	0.1388
River discharge ($Q_{R.Discharge}$)	0.0596
Groundwater exploitation ($Q_{Exploitation}$)	0.4397
Groundwater outflow ($Q_{Outflow}$)	0.0099
Total ($Q_{Excretion}$)	0.6480
$\triangle Q = Q_{Supply} - Q_{Excretion}$	0.1561

(Table 6) and the hydrogeological parameters of the mine (Table 8), respectively.

Figure 7a shows that the phreatic water quality is in agreement with the hydrodynamic conditions of the Chenqi Basin. The entire trend radiates from the D.M. Mine to the surrounding area while the cumulative component index gradually decreases with distance. In addition, Fig. 7a shows that Category IV and V were mainly distributed within 0.3 km of the mine, where the hydraulic gradient is the largest and the actual flow velocity is less due to drainage of the mine. However, in Fig. 7b, the Category III, IV, and V water samples were mainly from within 0.3 to 0.4 km around the mine. This indicates a good fit between the macro-regression and 1D partial differential equations. Notably, the area of the 1D analytic solution partial differential equation is slightly larger than the area of the macro-regression equation. In addition, the boundary of the former is smoother than the latter. As shown in Fig. 7a, b, phreatic water quality is variously distributed in the Chenqi Basin. The water quality (Table 9) is considerably different in distance (x) for Lines A, B, and C.

As described above, the Chenqi Basin is in an area where groundwater recharges and discharges. The direction of recharge is from the northeast toward the southwest. Low hills in the eastern and northern parts are the main groundwater recharge area of the basin, and the Hailar River Valley in the southwest constitutes the basin's drainage channel. The distinct results between the macro-regression and the 1D partial differential equations can be attributed to the direction of recharge. In addition, considering the influence of the Mergel River, the hydraulic gradient is reduced, and the flow velocity is large as the discharge direction changes at the northern edge of the cone of depression. Thus, a considerable difference was demonstrated in the northern parts between Fig. 7a, b. However, the simulation results are consistent with the fitting results in other directions where the effects of recharge are less disruptive.

As shown in Fig. 7a, b, most of the phreatic water of the Chenqi Basin can be used for domestic purposes after treatment and disinfection. In addition, both Fig. 7a, b show that most the Category V water, where the water is unsuitable for domestic utilization without being treated or disinfected, was within 0.3–0.4 km of the D.M. Mine.

Quality Prediction of Mine Water by CEI

According to Formula 11, the evaluation results are related to when water quality can be predicted by the CEI. Further phreatic water quality predictions for the Chenqi Basin for the next 10 years (Fig. 7c) is forecasted by Formula 11, assuming that conditions remain unchanged. Influenced by several factors, such as the direction and velocity of phreatic water flow and the phreatic aquifer storage, the trend of phreatic water quality mainly spreads in two directions, west and northwest. The zone wherein the water is unaffected, which only spans a small area in the northeast of the Chenqi Basin in Fig. 7a, b, is significantly expanded in Fig. 7c. This expanded area is approximately 1.9–2.2 km from the mine to the Category III boundary. Lines B and C do not have any zone of unimpacted water, but Line A does not evidently change, and the unaffected zone is extended in the northern part of the Chenqi Basin.

If the drainage of D.M. Mine remains the same, it will cause the WQV to diffuse to the west of the mine (Table 10). Moreover, the speed of diffusion is higher in the southwest than in the west and northwest directions. This is consistent with the observation that the recharge–discharge direction of the Chenqi Basin is from the northeast to the southwest. In addition, administrations and regulators should focus on the Argun River's water quality in the future due to the diffusion of WQV, which may potentially threaten continued use of groundwater and surface water resources.

Uncertainty Analysis

Many factors can introduce uncertainty in water quality evaluations, including: (1) unrepresentative sampling; (2) questionable spatial and temporal representativeness due to seasonal fluctuations that can affect the hydrochemistry of surface water; and (3) uncertainties associated with supportive data, such as ignoring the potential effects of industrial

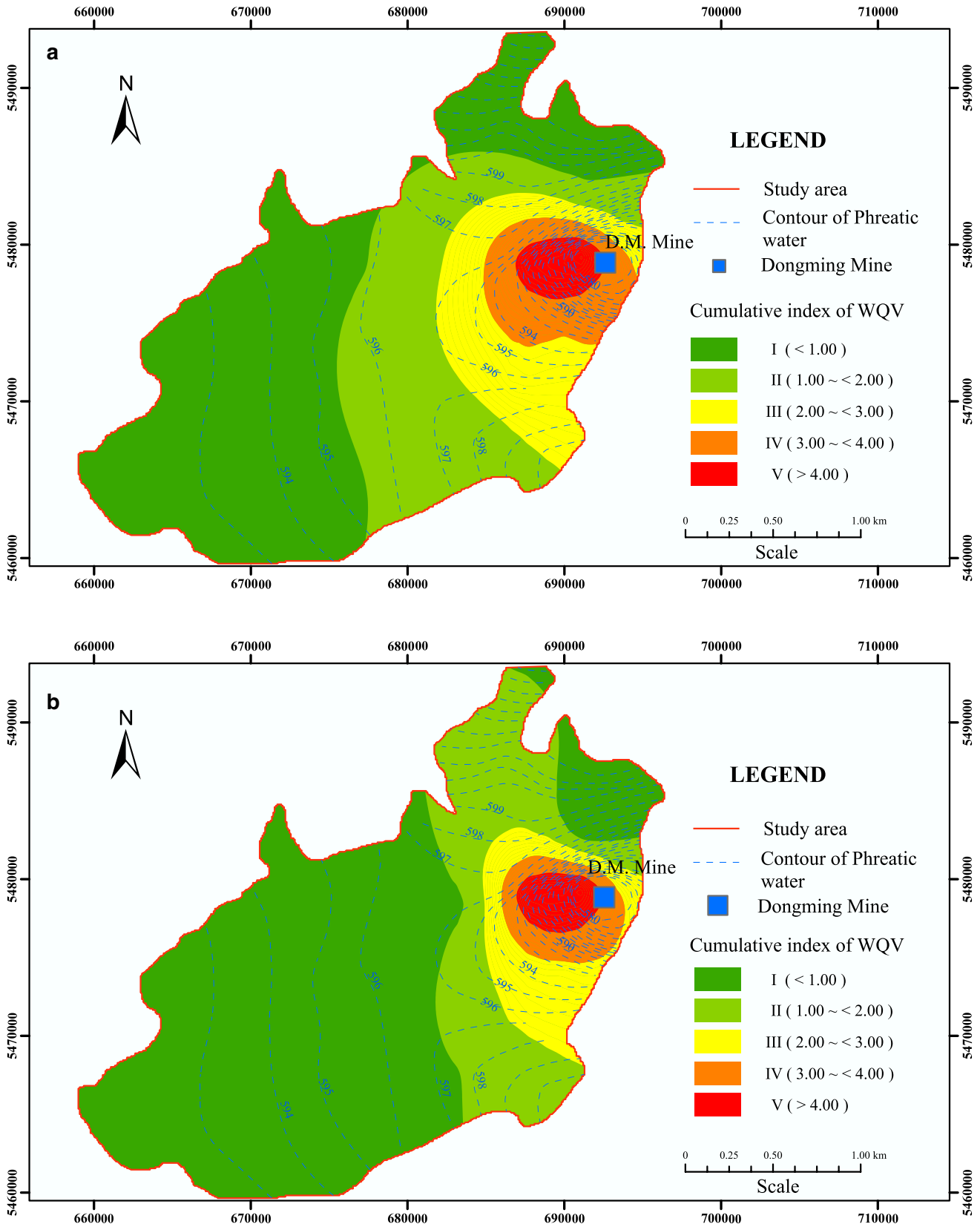

Fig. 7 Quality evaluation and prediction of mine water environment of Chenqi Basin. **a** Contour map of phreatic water quality by CEI. **b** Contour map of phreatic water quality by regression equation. **c** Contour map of phreatic water quality by CEI in 10 years

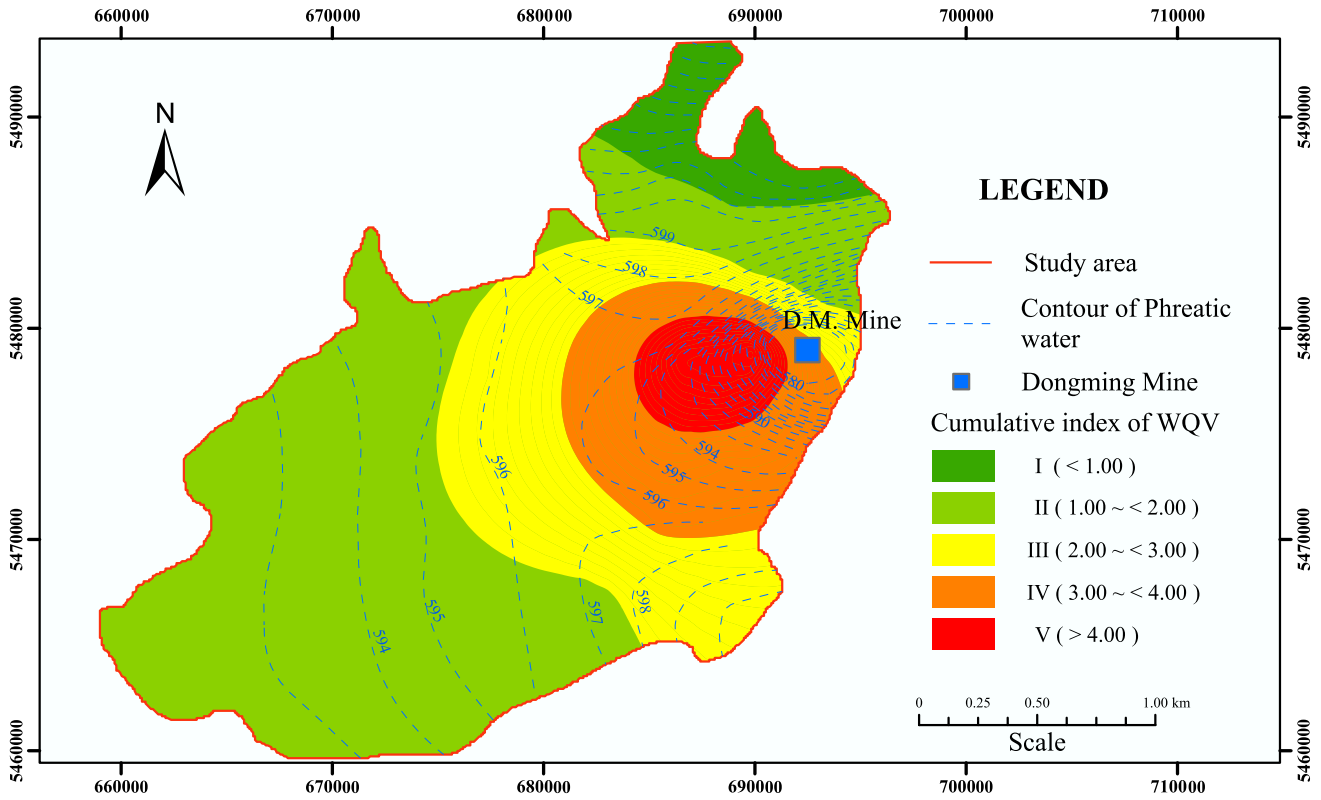

Fig. 7 (continued)

Table 8 Hydrogeological parameters of phreatic water in Chenqi Basin

Well	Thickness of quaternary(m)	Thickness of aquifer (m)	Drawdown (m)	Water inflow Q (m^3/d)	Unit discharge q (L/s·m)	Permeability coefficient K (m/d)	Hydraulic gradient I	Mean velocity u (m/d)
S1-1	81	75.55	3.24	4694.2	16.768	96.9	0.00156	0.5038
S1-2	78.3	75.85	1.37	5690.13	48.25	198.5		1.0322
S1-3	43.2	36.2	3.31	2992.03	10.466	57.93		0.3012
S1-4	50	48	2.48	1650.84	7.706	51.43		0.2674
S2-1	56	51	14.94	2706.74	2.097	52.5	0.00712	0.3710
S2-2	59.6	48.43	24.91	2159.64	1.004	95.6		0.6755
S2-3	50	24.13	4.13	3773.43	10.574	121.9		0.8614
S2-4	28	16.1	4.42	3191.96	8.36	142		1.0034
S3-1	36	34.8	12.57	1064.1	0.98	33.15	0.00172	0.1900
S3-2	20.1	16.45	11.46	1605.4	1.621	35.8		0.2052
S3-3	75.5	69.05	28.5	3955.65	1.61	173		0.9918
S3-4	76.6	70.95	2.03	5205.51	29.738	251		1.4390

Table 9 Evaluation of phreatic water quality of Chenqi Basin

Path	I	II	III	IV	V
Line A	> 0.8 km	0.5–0.8 km	0.3–0.5 km	0.1–0.3 km	0–0.1 km
Line B	> 1.3 km	0.9–1.3 km	0.6–0.9 km	0.4–0.6 km	0–0.4 km
Line C	> 2.2 km	1.2–2.2 km	0.6–1.2 km	0.2–0.6 km	0–0.2 km

sewage in some regions. Uncertainties can lead to water quality classification errors. To minimize errors induced by the preceding uncertainties, the following suggestions are made: (1) sampling efforts should target water flowing through the fractures and not the water in the wells; (2) samples must be spatially and temporally representative; (3) polluted water

Table 10 Prediction of phreatic water quality of Chenqi Basin in 10 years

Path	I	II	III	IV	V
Line A	> 1.2 km	0.8–1.2 km	0.5–0.8 km	0.2–0.5 km	0–0.2 km
Line B	–	> 1.3 km	0.9–1.3 km	0.6–0.9 km	0–0.6 km
Line C	–	> 1.4 km	0.7–1.4 km	0.3–0.7 km	0–0.3 km

sources, such as water from factories and municipal sewage, should be sampled to assess their potential effects.

Conclusions

In most parts of the Chenqi Basin, phreatic water can be used for domestic purposes after treatment and disinfection. The D.M. Mine water environment affects the groundwater table and water quality. Application of a regression equation and cumulative evaluation index to hydrochemical data from 12 samples revealed that the mine's current phreatic water quality is generally acceptable. If the mine maintains its present production, then it will significantly influence phreatic water quality in the future. Our findings suggest that mining would considerably affect the southwestern area of the Chenqi Basin but will have little effect on the northwest part, which will be controlled by the recharge and discharge conditions for at least the next 10 years.

Notably, this study can evaluate and forecast phreatic water quality attributed to mining, compensating for data errors caused by insufficient information. The findings also helped provide water quality data for a few aspects, which fit the actual situation well. Furthermore, PHREEQC, WASP5, and DYNHD5 can be used to simulate and analyse diffusion of WQV with various groundwater levels to make dynamic predictions of the phreatic water quality.

Acknowledgements The authors thank Dr. Peiyue Li for his constructive suggestions. This research was financially supported by the China National Scientific and Technical Support Program (2016YFC0801800), the China National Natural Science Foundation (41430318, 41272276, 41602262 and 41572222), Beijing Natural Science Foundation (8162036), and the National Geological Survey Program (DD20160266), Innovation Research Team Program of Ministry of Education (IRT1085) and State Key Laboratory of Coal Resources and Safe Mining. The authors gratefully acknowledge financial support from the China Scholarship Council (CSC). The authors also thank the editors and reviewers for their constructive input.

References

Andrade LN, Araujo SF, Matos AT, Henriques AB, Oliveira LC, Souza PP, Chagas P, Leão MMD, Amorim CC (2017) Performance of different oxidants in the presence of oxisol: Remediation of groundwater contaminated by gasoline/ethanol blend. Chem Eng J 308:428–437

Balintova M, Singovszka E, Vodicka R, Purcz P (2016) Statistical evaluation of dependence between pH, metal contaminants, and flow rate in the AMD-affected Smolnik Creek. Mine Water Environ 35(1):10–17

Bencer S, Boudoukha A, Mouni L (2016) Multivariate statistical analysis of the groundwater of Ain Djacer area (eastern Algeria). Arab J Geosci 9:248. https://doi.org/10.1007/s12517-015-2277-6

Chai TK (1981) Management of groundwater basin: theory and practice (translated by Wang BC). Geological Publ House, Beijing **(in Chinese)**

Fijani E, Moghaddam A, Tsai F, Tayfur G (2017) Analysis and assessment of hydrochemical characteristics of Maragheh-Bonab Plain aquifer, northwest of Iran. Water Resour Manage 31(3):765–780

Houillon N, Lastennet R, Denis A, Malaurent P (2016) Hydrochemical and hydrodynamic behavior of the epikarst at the Lascaux Cave (Montignac, France). EuroKarst 2016 Neuchâtel. Cham: Springer, p 319–326

IBM Corp. Released 2012. IBM SPSS Statistics for Windows, Version 21.0. Armonk, New York: IBM Corp

Jiries A, El-Hasan T, Al-Hweiti M, Seiler KP (2004) Evaluation of the effluent water quality produced at phosphate mines in central Jordan. Mine Water Environ 23(3):133–137

Lamhonwah D, Lafrenière M, Lamoureux S, Wolfe B (2017) Evaluating the hydrological and hydrochemical responses of a high arctic catchment during an exceptionally warm summer. Hydrol Process 31(12):2296–2313

Li P (2016) Groundwater quality in western China: challenges and paths forward for groundwater quality research in western China. Expos Health 8(3):305–310

Li P, Wu J, Qian H (2013) Assessment of groundwater quality for irrigation purposes and identification of hydrogeochemical evolution mechanisms in Pengyang County, China. Environ Earth Sci 69(7):2211–2225

Li P, Wu J, Qian H (2014) Origin and assessment of groundwater pollution and associated health risk: a case study in an industrial park, northwest China. Environ Geochem Health 36(4):693–712

Li P, Wu J, Yu H, Yang Z, Jing L, Yu P (2016) Hydrogeochemical characterization of groundwater in and around a waste water irrigated forest in the southeastern edge of the Tengger Desert, northwest China. Expos Health 8(3):331–348

Li P, Tian R, Xue C, Wu J (2017) Progress, opportunities and key fields for groundwater quality research under the impacts of human activities in China with a special focus on western China. Environ Sci Poll Res 24(15):13224–13234

Ling TY, Soo CL, Liew JJ, Nyanti L, Sim SF, Grinang J (2017) Application of multivariate statistical analysis in evaluation of surface river water quality of a tropical river. J Chem 2017:13. https://doi.org/10.1155/2017/5737452

Lu W, Bian Y, Li H (2006) Assessment and prediction of phreatic water quality in the catchment of Huanglong Industrial Site. Water Resour Protect 03:72–74 (Chinese)

Mahato MK, Singh PK, Tiwari AK, Singh AK (2016) Risk assessment due to intake of metals in groundwater of East Bokaro Coalfield, Jharkhand, India. Expos Health 8:265–275

Michael SW, Kenneth CH, Kelsey VF, Lynn P, Blair SB (2016) Water quality dynamics in an urbanizing subtropical estuary(Oso Bay, Texas). Marine Poll Bull 104(1–2):44–53

Mohammad A, Christoph R, Walker JP (2017) Statistical analysis of short-term water stress conditions at Riggs Creek Oz Flux tower site. Theor Appl Climatol 130(1–2):497–509

Noble TL, Lottermoser BG, Parbhakar-Fox A (2016) Evaluation of pH testing methods for sulfidic mine waste. Mine Water Environ 35(3):318–331

Qian C, Mu P (2016) Fuzzy comprehensive evaluation of groundwater quality based on principal component analysis. Water Resource Power 34:31–35 (Chinese)

Qian J, Wang L, Ma L, Lu Y (2016) Multivariate statistical analysis of water chemistry in evaluating groundwater geochemical evolution and aquifer connectivity near a large coal mine, Anhui, China. Environ Earth Sci 75:747

Rajmohan N, Patel N, Singh G, Amarasinghe U (2017) Hydrochemical evaluation and identification of geochemical processes in the shallow and deep wells in the Ramganga Sub-Basin, India. Environ Sci Poll Res 24(26):21459–21475

Rapantova N, Grmela A, Vojtek D, Halir J, Michalek B (2007) Ground water flow modelling applications in mining hydrogeology. Mine Water Environ 26(4):264–270

Senapaty A, Behera P (2012) Concentration and distribution of trace elements in different coal seams of the Talcher coalfield, Odisha. Int J Earth Sci Eng 5(5):80–87

Sun W, Wu Q, Liu H, Jiao J (2015) Prediction and assessment of the disturbances of the coal mining in Kailuan to karst groundwater system. Phys Chem Earth 89–90:136–144

Wu J, Li P, Qian H, Duan Z, Zhang X (2014) Using correlation and multivariate statistical analysis to identify hydrogeochemical processes affecting the major ion chemistry of waters: case study in Laoheba phosphorite mine in Sichuan, China. Arab J Geosci 7(10):3973–3982

Yihdego Y, Drury L (2016) Mine water supply assessment and evaluation of the system response to the designed demand in a desert region, central Saudi Arabia. Environ Monit Assess 188:619. https://doi.org/10.1007/s10661-016-5540-8

Environmental Systems Research Institute (2015) ArcGIS Release 10.3. Redlands